Carbohydrate Research 343 (2008) 2235–2242

Contents lists available at ScienceDirect

Carbohydrate Research

journal homepage: www.elsevier.com/locate/carres

# Theory and computation show that Asp463 is the catalytic proton donor in human endoplasmic reticulum α-(1→2)-mannosidase I

David Cantú [a], Wim Nerinckx [b], Peter J. Reilly [a,*]

[a] Department of Chemical and Biological Engineering, Iowa State University, Ames, IA 50011, USA
[b] Department of Biochemistry, Physiology and Microbiology, Ghent University, 9000 Ghent, Belgium

ARTICLE INFO

*Article history:*
Received 13 February 2008
Received in revised form 7 May 2008
Accepted 13 May 2008
Available online 6 June 2008

*Keywords:*
AutoDock
Catalytic residues
Endoplasmic reticulum mannosidase I
GH47
H++

ABSTRACT

It has been difficult to identify the proton donor and nucleophilic assistant/base of endoplasmic reticulum α-(1→2)-mannosidase I, a member of glycoside hydrolase Family 47, which cleaves the glycosidic bond between two α-(1→2)-linked mannosyl residues by the inverting mechanism, trimming $Man_9GlcNAc_2$ to $Man_8GlcNAc_2$ isomer B. Part of the difficulty is caused by the enzyme's use of a water molecule to transmit the proton that attacks the glycosidic oxygen atom. We earlier used automated docking to conclusively determine that Glu435 in the yeast enzyme (Glu599 in the corresponding human enzyme) is the nucleophilic assistant. The commonly accepted proton donor has been Glu330 in the human enzyme (Glu132 in the yeast enzyme). However, for theoretical reasons this conclusion is untenable. Theory, automated docking of α-D-$^3S_1$-mannopyranosyl-(1→2)-α-D-$^4C_1$-mannopyranose and water molecules associated with candidate proton donors, and estimation of dissociation constants of the latter have shown that the true proton donor is Asp463 in the human enzyme (Asp275 in the yeast enzyme).



## 1. Introduction

Endoplasmic reticulum α-(1→2)-mannosidase I (ERManI, EC 3.2.1.113) belongs to glycoside hydrolase family 47 (GH47).[1] It cleaves the glycosidic bond between two α-(1→2)-linked mannosyl residues by the inverting mechanism[1–3] and trims $Man_9GlcNAc_2$ to $Man_8GlcNAc_2$ isomer B.[2,3] Other GH47 α-(1→2)-mannosidases cleave other mannosyl residues to yield other products.[4]

Members of GH47 have an $(\alpha,\alpha)_7$-barrel fold (Fig. 1) and an active-site calcium ion[5–10] that is necessary for high enzyme activity and thermostability.[11] *Saccharomyces cerevisiae* and human ERManI enzymes are 35% similar in primary sequence,[2] but the amino acids involved in catalysis are practically the same.[6] Both enzymes have essentially the same crystal structure, and inhibitor binding causes little conformational change.[6,10]

In the inverting mechanism, an amino acid residue acting as a nucleophilic assistant/base helps a water molecule to perform a nucleophilic attack on the anomeric carbon. A second amino acid residue aids glycosidic bond cleavage by donating a proton to the glycosidic oxygen atom.[12] However, in ERManI the proton must be relayed by a water molecule, as no active-site carboxyl group is close enough to the glycosidic oxygen for direct proton donation. In addition, all three potential proton-donating groups coordinate water molecules (Fig. 2).[6] This is very unusual.

The conformation of the complexed substrate changes during cleavage. Human ERManI binds the inhibitors kifunensine and 1-deoxymannojirimycin in its subsite −1 in the unusual $^1C_4$ conformation.[6] The glycon of methyl 2-*S*-(α-D-mannopyranosyl)-2-thio-α-D-mannopyranoside (S-$Man_2$) is bound in the $^3S_1$ conformation, leading to the suggestion that its transition state is a $^3H_4$ conformer, intermediate between $^1C_4$ and $^3S_1$ conformers.[10] An automated docking study indicated that the substrate glycon in yeast ERManI must be in the $^1C_4$ conformation to enter the active site.[13] It then passes through $^3H_2$, $^OS_2$, $^{3,O}B$, and $^3S_1$ conformations to reach the putative $^3E$ transition-state conformer, structurally adjacent to the $^3H_4$ conformer.[13] After hydrolysis, the β-mannose molecule that had been the glycon finds itself successively in the $^1C_4$, $^1H_2$, and $B_{2,5}$ conformations before being expelled from the enzyme active site.[14]

It has been difficult to identify the ERManI catalytic proton donor and nucleophilic assistant/base. A crystal structure of the yeast enzyme with glycerol in the active site led to two hypotheses: (1) that Glu132 is the nucleophilic assistant to the water nucleophile, and that Asp275 or Glu435, probably the former, is the proton donor; and (2) alternatively and less likely that Glu435 is the nucleophilic assistant, with Glu132 being the proton donor.[5] A companion study with human ERManI again led to two hypotheses similar to those above: (1) that Glu599 (Glu435 in the corresponding yeast enzyme) is the nucleophilic assistant to Water5, with

* Corresponding author. Tel.: +1 515 294 5968; fax: +1 515 294 2689.
*E-mail address:* reilly@iastate.edu (P. J. Reilly).

0008-6215/$ - see front matter © 2008 Elsevier Ltd. All rights reserved.
doi:10.1016/j.carres.2008.05.026

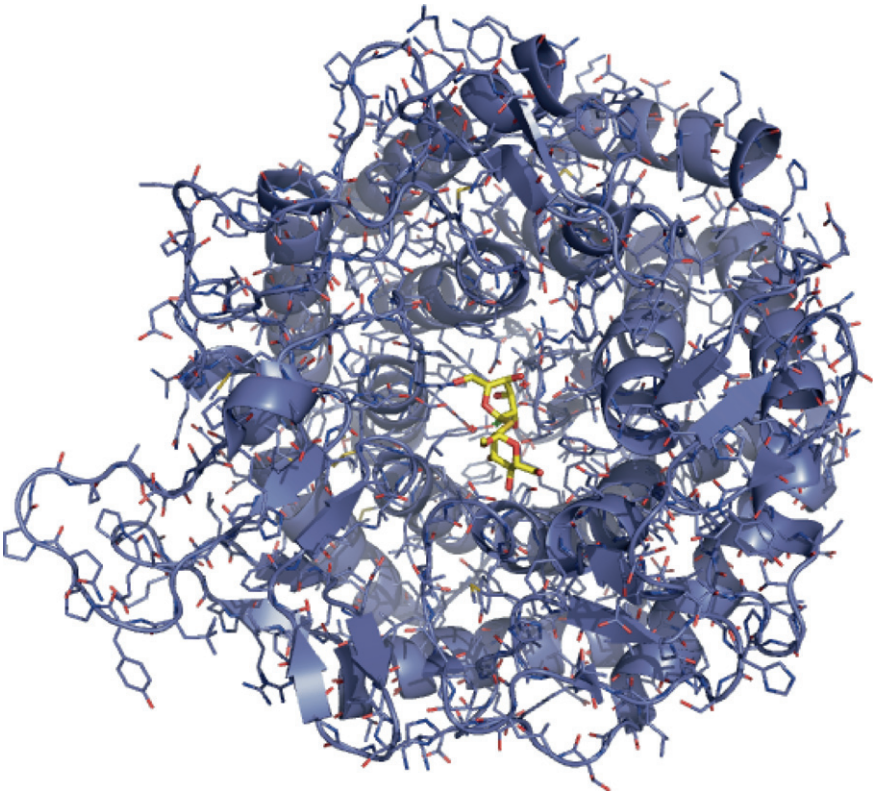

**Figure 1.** Human ERManI crystal structure 1X9D showing complexed S-$Man_2$.[10]

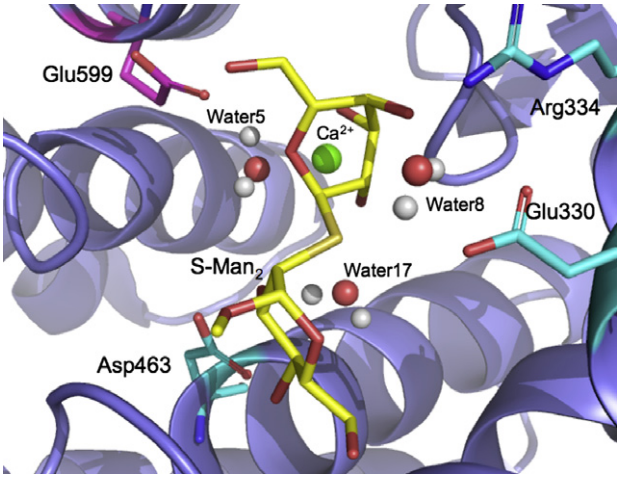


**Figure 2.** Crystal structure (with best-docked water molecules) of human ERManI active site. Pink: Glu599 nucleophile; blue: possible proton donors, either Asp463 or instead Glu330 paired with Arg334; yellow: S-$Man_2$; red: oxygen atoms; green: calcium ion. Water5 is between Glu599 and S-$Man_2$, Water8 is between Glu330 and S-$Man_2$, and Water17 is between Asp463 and S-$Man_2$.

Glu330 (Glu132) as the proton donor, transmitting a proton through Water8; and (2) that Asp463 (Asp275) is the nucleophilic assistant, with Water17 being the actual nucleophile, with Glu330 as the proton donor (Fig. 2).[6] A later study on human ERManI adopted the first hypothesis, suggesting that Arg334 (Arg136) contributed to the general acid function.[10] Work on *Hypocrea jecorina* and mouse GH47 enzymes with more capacious active sites yielded the same conclusions about the catalytic residues.[7,9] An automated docking study of yeast ERManI did not challenge Glu132 as the proton donor, acting through Water195, and identified Glu435 rather than Asp275 as the nucleophilic assistant to Water54.[15]

The nine invariant yeast ERManI acidic residues were mutated before any crystal structure was available. E214Q, D275N, E279Q, E435Q, and E503Q were not active, whereas D86N, E132Q, E438Q, and E526Q had <2% of the activity of wild-type ERManI.[11] A similar study on a GH47 enzyme from *Aspergillus saitoi* found the activity of E124Q (E132Q in yeast ERManI), E124D, D269N (D275N), D269E, E411Q (E435Q), and E411D as 0.02%, 0.2%, 0%, 1.9%, 0%, and 0.74% of the wild-type enzyme.[16] A third mutagenesis project conducted on human ERManI gave $k_{cat}/K_M$ values of 3.5%, 0.1%, 0.0005%, 0.006%, and 0.0003% of the wild-type value for E330Q (E132Q in yeast ERManI), D463N (D275N), E599Q (E435Q), E330Q/E599Q, and D463N/E599Q, respectively.[10]

In summary, identification of the ERManI catalytic proton donor and its associated water molecule is uncertain, because all three potential catalytic carboxyl groups coordinate water molecules, and because mutating each of these groups in yeast, *Aspergillus*, and human ERManI causes loss of all or nearly all activity. Therefore we have in this article considered the theory of GH catalysis and then the relative merits of putative proton donor/water systems, and have followed this with extensive use of computation, both by automated docking to determine orientations of substrate and water molecules, and by estimating p$K_a$'s of these groups.

## 2. Theory

### 2.1. Electrostatic transition-state stabilization in relation to *syn*- versus *anti*-protonation

Enzyme-catalyzed reactions are mediated by preferential stabilization of the transition state,[17] and electrostatic factors contribute the most to this stabilization.[18–20] At the transition state for the glycoside substitution reaction, the local charge distribution of

the glycon ring oxygen atom differs most substantially from that of the ground state or any local minimum conformation. In the latter cases, the ring oxygen atom always bears two fully occupied $sp^3$ lone pairs, whereas that in a glycoside transition state bears a fully occupied $sp^2$-hybrid and an electron-deficient $2p_z$ orbital that overlaps with the antibonding orbital of the anomeric carbon atom from the partially leaving or incoming groups. Since the ring oxygen atom is sterically relatively accessible, one expects that GHs will strategically position at least one electron-rich functional group (e.g., with a correctly oriented free electron pair) to intercept and stabilize this transient change in the local charge. A search for such a strategically positioned enzyme residue at the *syn*-A and/or *syn*-B space quadrants, axially above and/or underneath the ring oxygen atom of the glycon complexed in subsite −1 of GHs from different families, has indeed confirmed that *syn*-protonators, with their proton-donating carboxyl residues residing in the *syn*-half-space and close to the ring oxygen atom of the glycon, invariably use the conjugate base of the proton donor for electrostatic transition-state stabilization.[21] On the other hand, *anti*-protonators, their proton donors being in the *anti*-half-space and thus inherently far away from the ring oxygen, contain at least one electrostatic transition-state-stabilizing residue within the *syn*-half-space.

### 2.2. The Glu330/Water8 system as the putative proton donor

An indication that Glu330 in human ERManI (PDB code 1X9D) may not be the proton donor, with Water8 as the transferer of its proton to the glycosidic oxygen atom, is that this residue is in contact distance (3.05 Å) with Arg334 (Fig. 2). The Glu330/Arg334 system is expected to be zwitterionic, with Glu330 deprotonated and Arg334 protonated. Another counter-indication is that the possible proton-transferring Water8 is not semilaterally positioned versus the average ring plane of the S-$Man_2$ glycon occupying subsite −1 of the 1X9D complex structure, but it is instead near-orthogonally positioned. Indeed, a proton donor is expected to reside near-laterally, within the *anti*- or the *syn*-half-space (Fig. 3), to

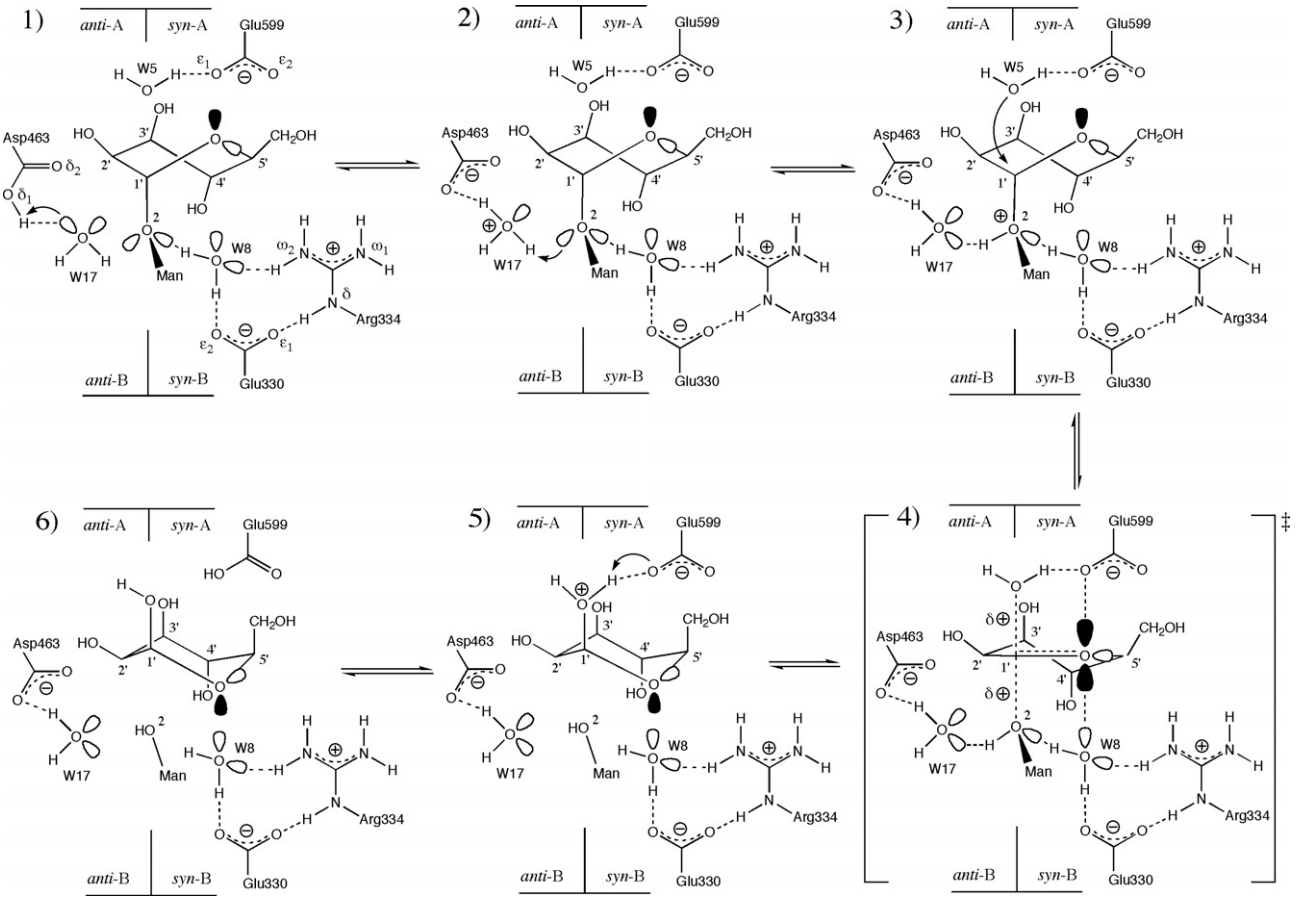


**Figure 3.** Six-panel illustration of the proposed substitution mechanism conducted by GH47 enzymes. These are idealized two-dimensional projections based on the actual three-dimensional arrangement within the human ERManI 1X9D crystal structure, and they are shown in relation to the *anti*-A, *anti*-B, *syn*-A, and *syn*-B space quadrants. The glycon ring oxygen's lone pair involved in the substitution process is indicated in black. When Asp463 is deprotonated, $O\delta_1$ and $O\delta_2$ of the carboxylate residue are equivalent because of resonance, as are $O\varepsilon_1$ and $O\varepsilon_2$ of Glu330 and Glu599 when the latter are deprotonated; $N\omega_1$ and $N\omega_2$ of Arg334's guanidino cation are also equivalent. *Panel 1*: Enzyme-occupied situation before the catalytic event. The D-mannosyl glycon resides in an ALPH-compliant $^3S_1$-like conformation, with the C1′–O2 glycosidic bond axial and in an antiperiplanar position versus the axial lone pair (in black) of the ring oxygen atom. A lone pair of the glycosidic oxygen atom is antiperiplanar to the C1′–O5′ bond, giving rise to the *exo*-anomeric effect. The proton on $O\delta_1$ of Asp463 is transferred to the nearby Water17. *Panel 2*: The lone pair of O2 that is involved in the *exo*-anomeric effect acquires a proton from the protonated Water17, which removes this stabilizing effect. The proton donor Asp463 as well as the proton-shuttling Water17 reside in the *anti*-half-space. This enzyme is therefore an *anti*-protonator. *Panel 3*: The ultimate substitution starts. Helped by Glu599 as nucleophilic assistant, Water5 axially attacks the glycosidic bond. *Panel 4*: The transition state with the D-mannosyl glycon in a $^3H_4$ (or the adjacent $^3E$) conformation. The transient $2p_z$ orbital (in black) of the ring oxygen atom, overlapping with the breaking and forming bonds, is electron-deficient and is locally accessible by the enzyme. It is electrostatically stabilized from *syn*-A by $O\varepsilon_1$ of Glu599, and from *syn*-B by a lone pair from Water8. This water molecule is oriented in the shown position by hydrogen bonding to the remaining lone pair of the glycosidic oxygen atom and to $O\varepsilon_2$ of Glu330, and by a hydrogen bond from $N\omega_2$ of Arg334 to its other lone pair. *Panel 5*: End of the anomeric substitution. The D-mannose product's end conformation is the $^1C_4$ inverted chair. The hydroxyl group of the newly formed hemiacetal is still protonated, and the nearby $O\varepsilon_1$ of Glu599 finally acquires this proton. *Panel 6*: End situation of the catalytic event. The products subsequently leave the enzyme, and the liberated D-mannose molecule will flip into the ground-state $^4C_1$ chair in an independent conformational process. Finally, a proton exchange between Glu599 and Asp463 will reset the enzyme for a next catalytic cycle.

the glycon occupying subsite −1, as observed in many GH families.[22,23] Instead, it is the observed oxygen atom of Water17, associated with the former putative nucleophilic assistant Asp463, that is clearly lateral and *anti*-positioned, at 3.60 Å from S-$Man_2$'s glycosidic sulfur atom, which fits with the following observations.

### 2.3. The occurrence of the *exo*-anomeric effect in relation to *syn*- versus *anti*-protonation

In the 1X9D complex, the S-$Man_2$ O5′–C1′–S2–C2 dihedral angle is 73°, and therefore the thioglycosidic bond displays the *exo*-anomeric effect.[24] The same is observed for the O5′–C1′–O2–C2 dihedral angles in the best docked $Man_2$ ligands of this study. This effect stabilizes the glycosidic bond by about 4 kcal/mol,[25] which is mainly attributed to a hyperconjugative overlap of the O5′–C1′ antibonding orbital with an antiperiplanar-oriented lone-pair orbital lobe of the glycosidic heteroatom. This lobe is semilaterally positioned versus the glycon and in 1X9D is directed toward Water17, which resides in the *anti*-half-space (Fig. 3). It indicates that GH47 enzymes are *anti*-protonators, since protonation of the lone pair that is involved in the *exo*-anomeric effect automatically removes this stabilizing effect en route to the transition state. Oligosaccharides that span subsites −1 and +1 of *anti*-protonating GHs appear to always show their glycosidic bonds in conformations dictated by the *exo*-anomeric effect, with protonation of the lone pair that is involved in it, whereas those complexed in *syn*-protonating enzymes consistently do not show an *exo*-anomeric effect conformation at this subsite junction.[21]

In the case of *anti*-protonators, where the proton donor is situated semilaterally versus the sugar's average ring plane and rather near to the C2 atom of the sugar entity in subsite −1, the protonation necessarily has to occur on a lone pair of the glycosidic oxygen that is also semilaterally positioned, and this is automatically so when the glycosidic bond resides in a conformation that conforms to the *exo*-anomeric stabilizing effect. In the case of *syn*-protonators, where the proton donor is again situated semilaterally versus the sugar's average ring plane but is now rather near to the glycon ring oxygen atom, the β- or α-scissile glycosidic bond must turn clockwise or counterclockwise, respectively, out of the *exo*-anomeric effect conformation, thereby bringing a lone pair of the glycosidic oxygen atom into a semilateral position that is within reach of the *syn*-proton donor. This is a consequence of the original *syn*- versus *anti*-protonation insight by Heightman and Vasella.[22] It is also derived from the correlation of the non-*exo*-anomeric effect conformation of the glycosidic bond versus *syn*-protonation that can be repeatedly observed in crystal structures with Michaelis complexes spanning subsites −1 and +1 of *syn*-protonating glycoside hydrolases, such as in PDB structures 1QJW, 1OVW, 2QZ3, 1W2U, and 1ITC. On the other hand, the *exo*-anomeric effect is preserved with Michaelis complexes of *anti*-protonators, such as in PDB structures 1VO3, 1JYW, 1IEX, 4A3H, 1KWF, and 1CKX.

### 2.4. The Asp463/Water17 system as the putative proton donor

The $O\delta_1$ atom of the carboxyl group of Asp463 in human ERManI (1X9D)[10] is 3.70 Å from Water17 and 2.72 Å from the C4–O atom of the D-mannosyl moiety in subsite +1 (Fig. 2). Furthermore, Water17 is in contact distance to the lone pair involved in the *exo*-anomeric effect. The $O\delta_2$ atom of Asp463 is 4.24 Å from Water17 and 2.51 Å from the C3–O atom of this D-mannosyl residue. It is thus possible that Asp463 has a double role: (1) as an indirect proton donor, through Water17, to the glycosidic oxygen atom; and (2) as an interactor with the D-mannosyl residue occupying subsite +1.

If Water17 is indeed the transmitter of the proton from Asp463 to the substrate glycosidic oxygen atom, then one of its hydrogen atoms should be pointing toward this glycosidic oxygen atom while one of its lone pairs should be directed toward Asp463. One purpose of this work is to investigate the specific orientation of Water17 by means of automated docking experiments.

### 2.5. The role of the Glu330/Arg334/Water8 system

Within the *syn*-A space quadrant of the glycon in the S-$Man_2$ complex with human ERManI, $O\varepsilon_1$ of the nucleophilic assistant Glu599 is 3.54 Å from, and nearly axial to, the glycon ring oxygen atom, a situation analogous to many other *anti*-protonating α-GHs (Figs. 2 and 3).[21] At *syn*-B the Water8 oxygen atom is 4.32 Å from and axial to the ring oxygen atom. It should be noted that the glycon in the observed complex resides in a $^3S_1$ conformation, whereas in passing to a $^3H_4$- or $^3E$-type transition state this ring oxygen atom will move even closer to Water8. For Water8 to be an electrostatic transition-state stabilizer rather than the transmitter of a donated proton, one of its free electron pairs should be directed toward the ring oxygen atom so that it can intercept and stabilize the transient electron-deficient $2p_z$ orbital. This may very well be so, since the nearest neighbors of the Water8 oxygen atom are (1) the ligand's glycosidic sulfur atom at 3.23 Å; (2) $O\varepsilon_2$ of the likely deprotonated Glu330 at 2.63 Å, each to where the hydrogen atoms of Water8 may very well be pointing; as well as (3) $N\omega_2$ of the likely protonated Arg334 at 2.73 Å, to where the other lone pair of Water8 may be directed. This suggests that the role of the conserved Glu330/Arg334 system is to specifically orient Water8 for electrostatic transition-state stabilization of the glycon ring oxygen atom. If this rationale is correct, then it should be possible to reproduce this specific orientation of the hydrogen atoms of Water8 by automated docking, which is the other purpose of this work.

## 3. Computational methods

### 3.1. Plan of work

This project uses automated docking, which we have used previously with yeast ERManI[13–15] and with several other GHs and lectins, to more surely identify the catalytic proton donor in ERManI. Here, we docked substrates and water molecules into the human ERManI crystal structure to determine whether Glu330 paired with Arg334 is mediating proton donation through Water8, or whether it is Asp463 mediating proton donation through Water17. We have supplemented this work with computation to determine the probable protonation states of the putative catalytic residues.

### 3.2. Automated docking

We docked ligands using AutoDock 3.0[26] into the human ERManI crystal structure 1X9D.[10] The normal ligands used were α-D-mannopyranosyl-(1→2)-α-D-mannopyranose ($Man_2$), with its glycon and aglycon having $^3S_1$ and $^4C_1$ conformations, respectively, and a water molecule. Ligands were given the desired three-dimensional conformation and hydrogen atoms were added using PCModel (Serena Software, Bloomington, IN, http://www.serenasoft.com). $Man_2$ was pair-fitted with S-$Man_2$ in the enzyme active site with PyMOL (DeLano Scientific, Palo Alto, CA, http://pymol.sourceforge.net) so that both had the same coordinates. Then, charges were assigned to the ligands using GAMESS.[27] AutoTors in the AutoDock suite was used to define the ligand torsions. The designations of nonpolar hydrogen atoms, those bonded to carbon atoms, were changed so that the program could differentiate them from the polar hydrogen atoms bonded to oxygen atoms.

Hydrogen atoms were added to the enzyme using the WHAT IF[28] webpage. Charges of each atom were added, as well as solvation parameters. Nonpolar hydrogen atoms were specified. Grid maps with 0.375 Å spacing were created using AutoGrid in the AutoDock package.

To calculate the electron-affinity map, AutoGrid assumes that full and fractional charges on atoms are located at their centers. However, this is not so with heteroatoms containing a free electron pair. Oxygen atoms have two local negative charges, both somewhere near the centers of the lone pairs. It is remarkable that AutoDock/AutoGrid and other empirical modeling programs yield reliable dockings, even with such a serious deviation from the real situation.

AutoDock was used to find ligand docking positions in the enzyme active site and to calculate the total binding energy ($E_{\text{Total}}$), while holding the enzyme but not the ligands rigid. This was a two-step process, a global search using the Lamarkian genetic algorithm option followed by a Solis and Wets local search.[26] Our global searches were stopped after 1000 runs, yielding 1000 possible ligand locations in the enzyme. These were gathered into clusters so that all members of each cluster were within a root-mean-squared deviation (RMSD) of 1 Å of all other members. After the global search, the best fitted member of each of six clusters with significant numbers of members was chosen based on its conformation and location in the enzyme active site, and on its $E_{\text{Total}}$ value. Then, to enhance dockings, local minimizations were done on each of the six ligands found by the global search.[13] The optimally docked ligand was chosen from the six locally minimized ones based on the criteria stated above, and final values of the intermolecular energy, $E_{\text{Inter}}$, between ligand and enzyme were determined. This rigorous docking procedure characteristically yields much more negative $E_{\text{Inter}}$ values than those normally attained with AutoDock.

To confirm that AutoDock places molecules in the correct location in the active site of ERManI, we docked S-$Man_2$ and measured the RMSD between docked and crystal-structure ligands as 0.23 Å. Also, we docked a Water8 molecule and a Water17 molecule in ERManI with S-$Man_2$ bound in the active site, yielding distances between the oxygen atoms of the docked and crystal water structures of 0.44 Å and 0.53 Å, respectively.

Following this, each regular docking set had the same protocol: S-$Man_2$ in the human ERManI structure was removed and $Man_2$ was docked, followed by a water molecule, either Water8, adjacent to Glu330 and Arg334, or Water17, adjacent to Asp463, into the enzyme active site. This was followed by redocking $Man_2$ and then the water molecule.

In the first docking set, $Man_2$ and Water8 were docked in ERManI while varying the protonation states of Glu330, a putative proton donor, and Arg334, adjacent to it. The enzyme's putative nucleophilic assistant, Glu599, was deprotonated in all dockings, as was Asp463, the other putative proton donor. All the water molecules in the enzyme were removed except for Water5, which is coordinated by Glu599 and is maintained in its crystal-structure position. There are fifteen possible ways in which Glu330 and Arg334 can be protonated or deprotonated: four in which both are deprotonated ($Glu^-/Arg^{0a}$, $Glu^-/Arg^{0b}$, $Glu^-/Arg^{0c}$, and $Glu^-/Arg^{0d}$), where a proton has been abstracted from each of four positions of the two Arg334 amino groups, one in which Glu330 is deprotonated and Arg334 is protonated ($Glu^-/Arg^+$), eight in which Glu330 is protonated and Arg334 is deprotonated ($Glu^{0e}/Arg^{0a}$, $Glu^{0e}/Arg^{0b}$, $Glu^{0e}/Arg^{0c}$, $Glu^{0e}/Arg^{0d}$, $Glu^{0f}/Arg^{0a}$, $Glu^{0f}/Arg^{0b}$, $Glu^{0f}/Arg^{0c}$, and $Glu^{0f}/Arg^{0d}$), and two in which both are protonated ($Glu^{0e}/Arg^+$ and $Glu^{0f}/Arg^+$), where a proton is found on each of two Glu330 oxygen atoms.

In the second docking set, $Man_2$ and Water17 were docked in ERManI with varying protonation states of Asp463, the other putative proton donor. Glu330 and Glu599 were deprotonated and Arg334 was protonated. Water5 and Water8 were located in their crystal-structure positions. There are three possible ways in which Asp463 can be deprotonated or protonated ($Asp^-$, $Asp^{0a}$, and $Asp^{0b}$), and all three were investigated.

### 3.3. Computational determination of p$K_a$ values of potential catalytic residues

The web-accessible program H++ automatically computes p$K_a$ values of dissociable groups in macromolecules.[29,30] It was used here to estimate the p$K_a$'s of Glu330, Arg334, Asp463, and Glu599 in the unliganded human ERManI crystal structures 1FMI[6] and 1X9D[10] and in the latter crystal structure when it was complexed with S-$Man_2$. H++ requires a contiguous amino acid sequence; however, 1X9D lacks the coordinates of Pro676, which is near the surface on the opposite side of the enzyme from the active site. These coordinates in 1X9D were restored by taking those from an automatic overlap with 1FMI using the Swiss-PDB viewer.[31] Conversely, 1FMI lacks the coordinates of Trp389 and Thr390, located on the enzyme surface 15 Å from its active site. The unbroken sequence of the structure was restored by using the coordinates of these residues from an automatic overlap with 1X9D.

The H++ program can process only one ligand within a macromolecule, so all water molecules were removed (solvation effects are implicitly accounted for by the program's methodology), as were $SO_4^{2-}$, $Ca^{2+}$, and 1,4-butandiol (when it was present). Removal of $Ca^{2+}$, even though it is essential for ERManI recognition of the glycon through the latter's C2′–OH and C3′–OH groups, should not drastically influence the p$K_a$ values of the residues (the putative proton donors Glu330 and Asp463, Arg334, and the putative nucleophilic assistant Glu599), since $Ca^{2+}$ is sufficiently far away from them. The ligand atom names were indicated as LIGAND to be recognized as such by H++. Default physical conditions were used: a salinity of 0.15, internal and external dielectric constants of 6 and 80, respectively, and a pH of 6.5.

## 4. Results and discussion

### 4.1. Docking of $Man_2$ and Water8 with different Glu330 and Arg334 protonation states

The first docking set (Tables 1 and 2 and Supplementary data) was designed to study the effect of the different protonation states of Glu330 and Arg334 while docking $Man_2$ and Water8, the latter located between these two amino acid residues and $Man_2$. Many of these protonation states, as when Glu330 is unprotonated, requiring Arg334 to be the proton donor, are unlikely in practice but serve as controls to validate ligand dockings that could indicate successful proton donation to the glycosidic oxygen atom. Exploring all possible protonation states also tests the ability of AutoDock to differentiate between viable and nonviable ones.

A number of criteria can be employed to choose successful protonation states. Among them are (1) significantly negative sums of $E_{\text{Inter}}$ for $Man_2$ and Water8 docking; (2) low RMSDs of docked $Man_2$ to crystal-structure $Man_2$; (3) low distances between the docked oxygen atom in Water8 and the crystal-structure Water8 oxygen atom (no protons appear in crystal-structure Water8); (4) intermediate distances between the nearer proton in docked Water8 and the docked glycosidic oxygen atom (O2 of $Man_2$), between the proton in Glu330 and the docked Water8 oxygen atom, between the oxygen atom of docked Water8 and the ring oxygen atom of the glycon (O5′ of docked $Man_2$), and between a proton in Arg334 and the docked Water8 oxygen atom; and (5) a correctly docked

**Table 1**
Energies and distances from docking $Man_2$ and Water8 into the human ERManI active site

| Charge status | | $Man_2$ docking | | Water8 docking | | Distance, Å | | | |
|---|---|---|---|---|---|---|---|---|---|
| Glu330 | Arg334 | $E_{Inter}$, kcal/mol | RMSD, Å | $E_{Inter}$, kcal/mol | Distance, Å | H(Water8)–O2($Man_2$) | H(Glu330)–O(Water8) | O(Water8)–O5′($Man_2$) | H(Arg334)[h]–O(Water8) |
| – | $0^{a}$ | −151.2 | **1.18**[g] | −49.6 | **1.73** | 3.60 | – | **5.21** | **4.07** |
| – | $0^{b}$ | **−151.3** | 0.99 | **−37.6** | **1.73** | 1.98 | – | 4.19 | 3.57 |
| – | $0^{c}$ | −161.7 | **1.29** | −34.3 | 0.51 | 3.36 | – | 4.20 | 1.87 |
| – | $0^{d}$ | −162.0 | 0.80 | −33.1 | 0.40 | 3.31 | – | 4.57 | 2.18 |
| – | + | **−141.6** | 0.87 | **−33.4** | 0.38 | 3.47 | – | 4.44 | 1.65 |
| $0^{e}$ | $0^{a}$ | −182.6 | 0.94 | −32.9 | **1.81** | 1.91 | 2.33 | 4.33 | **4.61** |
| $0^{e}$ | $0^{b}$ | −186.4 | 0.94 | −41.5 | **2.55** | 2.07 | 2.81 | 4.60 | **4.37** |
| $0^{e}$ | $0^{c}$ | **−149.0** | 1.09 | **−32.6** | 0.38 | 2.45 | 1.73 | 4.23 | 2.19 |
| $0^{e}$ | $0^{d}$ | −152.4 | 1.06 | −39.2 | **1.32** | 1.68 | 1.99 | 3.99 | 3.16 |
| $0^{e}$ | + | −169.3 | 1.10 | −31.9 | 0.41 | 2.45 | 1.82 | 4.76 | 1.81 |
| $0^{f}$ | $0^{a}$ | **−148.2** | **1.24** | **−30.6** | 0.54 | **4.03** | 2.85 | 4.14 | 2.69 |
| $0^{f}$ | $0^{b}$ | **−150.6** | 1.08 | **−36.2** | **1.68** | 1.82 | **4.21** | 4.10 | 3.52 |
| $0^{f}$ | $0^{c}$ | **−140.6** | 0.99 | **−33.7** | 0.27 | 3.23 | 3.04 | 4.28 | 2.09 |
| $0^{f}$ | $0^{d}$ | −162.6 | 0.87 | −35.1 | 0.37 | 3.51 | 3.09 | 4.65 | 2.17 |
| $0^{f}$ | + | −167.8 | **1.25** | −35.0 | **2.13** | 1.74 | **4.78** | 3.90 | **4.03** |

[a] Proton missing in more distant position of Arg334 $N\omega_2$ atom.
[b] Proton missing in nearer position of Arg334 $N\omega_2$ atom.
[c] Proton missing in nearer position of Arg334 $N\omega_1$ atom.
[d] Proton missing in more distant position of Arg334 $N\omega_1$ atom.
[e] Proton associated with Glu330 $O\varepsilon_2$ atom missing.
[f] Proton associated with Glu330 $O\varepsilon_1$ atom missing.
[g] Bolded numerals signify values that lessen possibility of proton donation.
[h] Distance is that to the nearer available proton bound to Arg334 $N\omega_2$ atom.

**Table 2**
Orientations from docking $Man_2$ and either Water8 or Water17 into the human ERManI active site

| Protonation state | $\phi$, degrees[a] | $\psi$, degrees[b] | Comments |
|---|---|---|---|
| $Glu^{-}/Arg^{0a}$ | **122.9**[c] | −169.7 | Water8 proton aimed at $Man_2$ O5′ |
| $Glu^{-}/Arg^{0b}$ | **115.9** | −145.5 | Water8 proton aimed at $Man_2$ O5′ |
| $Glu^{-}/Arg^{0c}$ | **124.2** | −168.7 | Water8 lone pair mainly oriented to $Man_2$ O5′; may improve with $^3H_4$ transition-state conformation |
| $Glu^{-}/Arg^{0d}$ | 81.8 | −146.1 | Water8 lone pair mainly oriented to $Man_2$ O5′; may improve with $^3H_4$ transition-state conformation |
| $Glu^{-}/Arg^{+}$ | 72.8 | −150.8 | Water8 lone pair mainly oriented to $Man_2$ O5′; may improve with $^3H_4$ transition-state conformation |
| $Glu^{0e}/Arg^{0a}$ | **117.8** | −158.5 | Water8 proton aimed at $Man_2$ O2, **but misaligned lone pairs of Water8 and $Man_2$O2**[d] |
| $Glu^{0e}/Arg^{0b}$ | **107.6** | −150.4 | **Misoriented Water8** |
| $Glu^{0e}/Arg^{0c}$ | **108.3** | −164.5 | Water8 lone pair mainly oriented to $Man_2$ O5′; may improve with $^3H_4$ transition-state conformation |
| $Glu^{0e}/Arg^{0d}$ | **122.7** | −166.8 | Water8 lone pair mainly oriented to $Man_2$ O5′; may improve with $^3H_4$ transition-state conformation |
| $Glu^{0e}/Arg^{+}$ | 66.9 | −152.1 | **Water8 misoriented for transition-state stabilization**; oriented correctly for protonation by **Glu330 or** Arg334 |
| $Glu^{0f}/Arg^{0a}$ | **121.2** | −162.7 | **Misoriented Water8** |
| $Glu^{0f}/Arg^{0b}$ | **118.5** | −169.5 | **Misoriented Water8** |
| $Glu^{0f}/Arg^{0c}$ | **110.2** | −165.7 | **Misoriented Water8** |
| $Glu^{0f}/Arg^{0d}$ | 72.8 | −142.1 | **Misoriented Water8** |
| $Glu^{0f}/Arg^{+}$ | **121.4** | −164.5 | **Misoriented Water8** |
| $Asp^{-}$ | 72.7 | −149.9 | **Water17 lone pair not oriented to Asp463** |
| $Asp^{0a}$ | 79.8 | −152.4 | Favorable orientation for Asp463 proton transfer to Water17 |
| $Asp^{0b}$ | 79.5 | −154.3 | **Misoriented Water17** |

[a] $\phi$ = O5′–C1′–O2–C2.
[b] $\psi$ = C1′–O2–C2–C1.
[c] Bold in $\phi$ and $\psi$ columns signifies that ligand is not in *exo*-anomeric state, but instead is in a near-eclipsed conformation.
[d] Bold in Comments column signifies traits that lessen possibility of proton donation.

Water8 orientation. Proton donation by the Glu330/Arg334/Water8 system is suggested if one of Water8's protons is aimed at the docked $Man_2$ glycosidic oxygen atom and its oxygen atom is facing Glu330 and Arg334. Ability to electrostatically stabilize the transient and electron-deficient $2p_z$ orbital of the O5′ atom at the transition state is suggested if a lone pair of the oxygen atom in Water8 is aimed at it.

Sums of $E_{Inter}$ values for $Man_2$ and Water8 docking range from −174.3 to −227.9 kcal/mol (Table 1). Sums less negative than ~190 kcal/mol are unlikely to indicate successful proton donation. These are generated by the protonation states $Glu^{-}/Arg^{0b}$, $Glu^{-}/Arg^{+}$, $Glu^{0e}/Arg^{0c}$, $Glu^{0f}/Arg^{0a}$, $Glu^{0f}/Arg^{0b}$, and $Glu^{0f}/Arg^{0c}$.

RMSD values of docked $Man_2$ to crystal-structure S-$Man_2$ range from 0.80 to 1.29 Å (Table 1). Relatively large RMSD values (greater than ~1.1 Å) when ERManI is in the $Glu^{-}/Arg^{0a}$, $Glu^{-}/Arg^{0c}$, $Glu^{0f}/Arg^{0a}$, and $Glu^{0f}/Arg^{+}$ protonation states lessen their likelihood of proton donation compared to those with lower RMSD values.

Docking of Water8 yields two different ranges of distances (0.27–0.54 Å and 1.32–2.55 Å) between their docked and crystal-structure oxygen atoms (Table 1). Protonation states, such as $Glu^{-}/Arg^{0a}$, $Glu^{-}/Arg^{0b}$, $Glu^{0e}/Arg^{0a}$, $Glu^{0e}/Arg^{0b}$, $Glu^{0e}/Arg^{0d}$ $Glu^{0f}/Arg^{0b}$, and $Glu^{0f}/Arg^{+}$, having distances in the second range, are unlikely to successfully donate a proton through Water8 to the glycosidic oxygen atom.

The distances (1) between the nearer proton of docked Water8 and the O2 atom of docked $Man_2$ range between 1.68 and 4.03 Å; (2) those between the docked Water8 oxygen atom and the proton associated with the $O\varepsilon_2$ atom in crystal-structure Glu330 are from 1.73 to 4.78 Å; (3) those between the oxygen atom of docked Water8 and the O5′ atom in docked $Man_2$ range from 3.90 to

5.21 Å; and (4) those between the docked Water8 oxygen atom and the nearer proton associated with the $N\omega_2$ atom in crystal-structure Arg334 range from 1.65 to 4.61 Å (Table 1). Values of >4 Å in the first two cases indicate a lesser probability of successful proton donation from Glu330 to Water8 to the glycosidic oxygen atom, while values of >5 Å in the third case suggest that a lone pair of Water8 would be unlikely to electrostatically stabilize the glycon ring oxygen during the transition state, and values of >4 Å in the fourth case suggest a lessened ability of Arg334 to stabilize and orient Water8 or to donate a proton through it to the glycosidic oxygen atom. These criteria suggest that the protonation states $Glu^-/Arg^{0a}$, $Glu^{0e}/Arg^{0a}$, $Glu^{0e}/Arg^{0b}$, $Glu^{0f}/Arg^{0a}$, $Glu^{0f}/Arg^{0b}$, and $Glu^{0f}/Arg^+$ are less likely candidates for successful proton donation.

Also measured were the distances between the oxygen atom of crystal-structure Water5, the putative nucleophile, and the C1′ atom of docked $Man_2$, which it attacks, for the different protonation states. In all cases these values are in an acceptable range between 2.89 and 3.38 Å.

The ligand $\phi$ dihedral angle (O5′–C1′–O2–C2) should be about 70°, indicating the presence of the *exo*-anomeric effect. Furthermore, the orientation of Water8 is extremely important for proton donation. Its oxygen atom should face Glu330 and Arg334, one of its lone pairs needs to face the glycon ring oxygen atom of $Man_2$, and one of its protons should face the glycosidic oxygen atom. Only two protonation states, $Glu^-/Arg^{0d}$ and $Glu^-/Arg^+$, satisfy these criteria (Table 2 and Supplementary data).

Use of the criteria listed above suggests that only one of these fifteen protonation states, $Glu^-/Arg^{0d}$, is a good proton donor candidate. However, in that state Glu330 has no proton to donate and Arg334 is not positively charged, leaving no readily available proton for donation.

Chemical reasoning suggests that the Glu330/Arg334 system can donate a proton only from double-protonated systems such as $Glu^{0e}Arg^+$ and $Glu^{0f}Arg^+$, with the proton being donated by a protonated Glu330. However, its protonation is not predicted by H++, as will be noted below. With $Glu^{0e}Arg^+$, Water8 is oriented correctly for proton transfer, but it is misoriented for transition-state stabilization. $Glu^{0f}Arg^+$ fails many criteria necessary for successful proton donation.

### 4.2. Docking of $Man_2$ and Water17 with different Asp463 protonation states

$Man_2$ and Water17 were docked in the second set, with Asp463 in different protonation states (Tables 2 and 3 and Supplementary data). Five criteria are important here: (1) the sums of $E_{Inter}$ values for $Man_2$ and Water17 docking should be more negative than ~190 kcal/mol, as before; (2) RMSD values between crystal-structure and docked $Man_2$ should be less than ~1.1 Å, as before; (3) distances between oxygen atoms of crystal-structure and docked Water17 should be less than ~1.1 Å; (4) distances between a proton in docked Water17 and the O2 atom of docked $Man_2$ should be <4 Å, between a proton in Asp463 and the oxygen atom of docked Water17 should be <4 Å, and between the oxygen atom of crystal-structure Water8 and the O5′ atom of docked $Man_2$ should be <5 Å; and (5) docked Water17 should be oriented so that a proton is aimed at the O2 atom of docked $Man_2$ and a lone pair is facing Asp463.

Sums of $E_{Inter}$ values in $Asp^-$, $Asp^{0a}$, and $Asp^{0b}$ are −186.7, −193.9, and −193.4 kcal/mol, respectively (Table 3), less negative than in many cases when the protonation states of Glu330 and Asp334 are varied. The least negative energy sum occurs with $Asp^-$, the only state of the three in which proton donation is not possible.

In all three cases, the RMSDs of docked $Man_2$ relative to crystal-structure S-$Man_2$ are under 1.0 Å (Table 3). The distances between the oxygen atoms of crystal-structure and docked Water17 are ⩽1.1 Å. Distances between the nearer proton in docked Water17 and the O2 atom of docked $Man_2$ are ~3 Å, while those between the nearer proton in Asp463, when present, and the Water17 oxygen atom are ⩽3 Å, allowing proton donation from Asp463 through Water17 to the $Man_2$ glycosidic bond. Furthermore, distances between Water8's oxygen atom and the O5′ atom range between 4.41 and 4.83 Å, suggesting that Water8 can electrostatically stabilize $Man_2$ during the transition state. Distances between the oxygen atom of crystal-structure Water5 and the C1′ atom of docked $Man_2$ are between 3.06 and 3.30 Å in all three cases, an acceptable range.

The orientation in which Water17 docks indicates its probability of proton donation. With $Asp^-$ and $Asp^{0b}$, proton donation cannot occur because Water17 is not correctly oriented so that one of its hydrogen atoms is pointing toward the glycosidic oxygen atom while one of its lone pairs is directed toward Asp463 (Table 2 and Supplementary data). However, Water17 docks in the correct position and with the right orientation to donate a proton from $Asp^{0a}$.

These docking results suggest that the only protonation state of Asp463 eligible to donate a proton to the glycosidic oxygen atom of $Man_2$ is $Asp^{0a}$. Since the Glu330/Arg334 system has no protonation states that appear likely to be proton donors, Asp463 appears by docking analysis to be the actual proton donor in ERManI.

### 4.3. Determination of p$K_a$ values with H++

Finally, we used H++ to predict the p$K_a$ values and protonation states of the potential catalytic residues in human ERManI (Table 4). Glu330 and Arg334 have predicted p$K_a$'s of near zero and much

**Table 4**
Dissociation constants of active-site residues in human ERManI

| Residue | Crystal structure | | |
|---|---|---|---|
| | 1FMI | 1X9D | 1X9D–$Man_2$ |
| Glu330 | −1.9 | 0.6 | 1.7 |
| Arg334 | 26.9 | 25.8 | 23.4 |
| Asp463 | 8.5 | 9.3 | 13.1 |
| Glu599 | −9.0 | −8.5 | −15.0 |

**Table 3**
Results from docking $Man_2$ and Water17 into the ERManI active site

| Charge status | $Man_2$ docking | | Water17 docking | | Distance, Å | | |
|---|---|---|---|---|---|---|---|
| Asp463 | $E_{Inter}$, kcal/mol | RMSD, Å | $E_{Inter}$, kcal/mol | Distance, Å | H(Water17)–O2($Man_2$) | H(Asp463)–O(Water17) | O(Water8)–O5′($Man_2$) |
| – | −155.2 | 0.89 | −31.5 | 1.10 | 3.03 | – | 4.50 |
| 0[a] | −161.4 | 0.91 | −32.5 | 0.84 | 3.09 | 2.16 | 4.41 |
| 0[b] | −164.0 | 0.94 | −29.4 | 0.67 | 3.11 | 3.02 | 4.83 |

[a] Proton associated with Asp463 $\delta_2$ atom missing.
[b] Proton associated with Asp463 $\delta_1$ atom missing.

above 14, respectively, so at physiological pH's the former is deprotonated and the latter is protonated, to the extent that its protons are so strongly bound that they cannot be donated. The putative proton donor Asp463, with a predicted p$K_a$ in the basic range, appears to be mainly or completely protonated, while the putative nucleophilic assistant Glu599, with a predicted p$K_a$ greatly below zero, indeed appears to be completely deprotonated.

H++ uses single-structure continuum solvent methodology, giving an average p$K_a$ error of about one unit, with potentially larger errors at both very negative and very positive p$K_a$ values.[29] However, it should give reasonable estimates of whether a dissociable group is protonated or not at these extremes. It is clear that movement of amino acid side chains during substrate binding and catalysis can change their p$K_a$ values. However, Glu330, Asp334, Asp463, and Glu599 are all part of α-helices (Fig. 2) and therefore have low potential for movement. Furthermore, Arg334 is located one turn on an α-helix from Glu330 and will always face in the same direction as the latter despite any movement. These results further confirm, as predicted by theoretical considerations and confirmed by docking analysis, that Asp463 acts as the proton donor in human ERManI.

### 4.4. Non-suitability of Glu330 as the nucleophilic assistant/base

With Glu330 eliminated as the putative proton donor, the question arises as whether it could be the nucleophilic assistant instead of Glu599. Glu330 is on the opposite side of the ligand from Water5, the natural nucleophile, preventing contact between them. An alternative possibility is for Water8 to be the nucleophile with Glu330 as the nucleophilic assistant. This would require that GH47 members hydrolyze substrates through an internal $S_Ni$ substitution, with the leaving group departing and the nucleophile replacing it from the same side. Although such a mechanism is known,[32,33] the leaving group would need to be much better than the mannosyl residue here. Furthermore, a classical base-assistant system rather than the Glu330–Arg334 zwitterionic system would need to compensate for a highly oxocarbenium-type $S_Ni$ transition state.

## 5. Conclusions

We have conducted this project to clearly identify the proton donor in ERManI, and by extension in all GH47 α-1,2-mannosidases. This question has remained open because no carboxyl group is close enough to the C1′ atom of the glycon for direct proton transfer, and because all three carboxyl groups near the substrate's glycosidic bond coordinate water molecules. In summary, our theoretical, docking, and p$K_a$ prediction studies show that Asp463 is the proton donor in human ERManI. Theoretical considerations based on the ERManI crystal structure[10] indicate that GH47 enzymes are *anti*-protonators, and that Asp463 is the only potential proton donor located in the *anti*-quadrant of the ERManI active site. Only protonated Asp463 allows a water molecule to be positioned to donate a proton to the $Man_2$ glycosidic oxygen atom and to allow another water molecule to electrostatically stabilize the glycon ring oxygen atom of $Man_2$. Glu330 paired with Arg334 is not the proton donor because Glu330 is deprotonated, due to its proximity to Arg334. Arg334 cannot be the proton donor because even when positively charged, it binds protons too tightly for them to be released.

## Acknowledgments

D.C.'s visit from the Instituto Tecnológico y de Estudios Superiores de Monterrey (Mexico) to Iowa State University (ISU) occurred through a US National Science Foundation Research Experiences for Undergraduates program, and he was supported through ISU funding. He conducted the latter part of his work while an exchange student at the Ecole Polytechnique Fédérale de Lausanne (Switzerland). The authors thank Blake Mertz and Anthony Hill for their help in the initial docking runs, ISU for furnishing its computational facilities for this research, and Professor Arthur Olson of the Scripps Research Institute for supplying AutoDock.

## Supplementary data

Supplementary data associated with this article can be found, in the online version, at doi:10.1016/j.carres.2008.05.026.

## References

1. Coutinho, P. M.; Henrissat, B. Carbohydrate-Active Enzymes: An Integrated Database Approach. In *Recent Advances in Carbohydrate Bioengineering*; Gilbert, H. J., Davies, G. B., Henrissat, B., Svensson, B., Eds.; Royal Society of Chemistry: Cambridge, 1999; pp 3–12. http://www.cazy.org/.
2. Herscovics, A. *Biochim. Biophys. Acta* **1999**, *1426*, 275–285.
3. Herscovics, A. *Biochim. Biophys. Acta* **1999**, *1473*, 96–107.
4. Herscovics, A. *Biochimie* **2001**, *83*, 757–762.
5. Vallée, F.; Lipari, F.; Yip, P.; Sleno, B.; Herscovics, A.; Howell, P. L. *EMBO J.* **2000**, *19*, 581–588.
6. Vallée, F.; Karaveg, K.; Herscovics, A.; Moremen, K. W.; Howell, P. L. *J. Biol. Chem.* **2000**, *275*, 41287–41298.
7. Van Petegem, F.; Contreras, H.; Contreras, R.; Van Beeumen, J. *J. Mol. Biol.* **2001**, *312*, 157–165.
8. Lobsanov, Y. D.; Vallée, F.; Imberty, A.; Yoshida, T.; Yip, P.; Herscovics, A.; Howell, P. L. *J. Biol. Chem.* **2002**, *277*, 5620–5630.
9. Tempel, W.; Karaveg, K.; Liu, Z.-J.; Rose, J.; Wang, B.-C.; Moremen, K. W. *J. Biol. Chem.* **2004**, *279*, 29774–29786.
10. Karaveg, K.; Siriwardena, A.; Tempel, W.; Liu, Z.-J.; Glushka, J.; Wang, B.-C.; Moreman, K. W. *J. Biol. Chem.* **2005**, *280*, 16197–16207.
11. Lipari, F.; Herscovics, A. *Biochemistry* **1999**, *38*, 1111–1118.
12. Koshland, D. E. *Biol. Rev. Camb. Philos. Soc.* **1953**, *28*, 416–435.
13. Mulakala, C.; Nerinckx, W.; Reilly, P. J. *Carbohydr. Res.* **2006**, *341*, 2233–2245.
14. Mulakala, C.; Nerinckx, W.; Reilly, P. J. *Carbohydr. Res.* **2007**, *342*, 163–169.
15. Mulakala, C.; Reilly, P. J. *Proteins* **2002**, *49*, 125–134.
16. Tatara, T.; Lee, B. L.; Yoshida, T.; Takahashi, K.; Ichishima, E. *J. Biol. Chem.* **2003**, *278*, 25289–25294.
17. Pauling, L. *Chem. Eng. News* **1946**, *24*, 1375–1376.
18. Warshel, A. *Proc. Natl. Acad. Sci. U.S.A.* **1978**, *75*, 5250–5254.
19. Warshel, A. *Acc. Chem. Res.* **1981**, *14*, 284–290.
20. Warshel, A. *Computer Simulation of Chemical Reactions in Enzymes and Solutions*; Wiley: New York, 1991.
21. Nerinckx, W.; Desmet, T.; Piens, K.; Claeyssens, M. *FEBS Lett.* **2005**, *579*, 302–312.
22. Heightman, T. D.; Vasella, A. T. *Angew. Chem., Int. Ed.* **1999**, *38*, 751–770.
23. Nerinckx, W.; Desmet, T.; Claeyssens, M. *FEBS Lett.* **2003**, *538*, 1–7.
24. Pérez, S.; Marchessault, R. H. *Carbohydr. Res.* **1978**, *65*, 114–120.
25. Cramer, C. J.; Truhlar, D. G.; French, A. D. *Carbohydr. Res.* **1997**, *298*, 1–14.
26. Morris, G. M.; Goodsell, D. S.; Halliday, R. S.; Huey, R.; Hart, W. E.; Belew, R. K.; Olson, A. J. *J. Comput. Chem.* **1998**, *19*, 1639–1642. http://autodock.scripps.edu/.
27. Schmidt, M. W.; Baldridge, K. K.; Boatz, J. A.; Elbert, S. T.; Gordon, M. S.; Jensen, J. H.; Koseki, S.; Matsunaga, N.; Nguyen, K. A.; Su, S.; Windus, T. L.; Dupuis, M.; Montgomery, J. A., Jr. *J. Comput. Chem.* **1993**, *14*, 1347–1363. http://www.msg.chem.iastate.edu.
28. Vriend, G. *J. Mol. Graph.* **1990**, *8*, 52–56. http://swift.cmbi.ru.nl/whatif/.
29. Gordon, J. C.; Myers, J. B.; Folta, T.; Shoja, V.; Heath, L. S.; Onufriev, A. *Nucleic Acids Res.* **2005**, *33*, W368–W371. http://biophysics.cs.vt.edu/H++/.
30. Myers, J.; Grothaus, G.; Narayanan, S.; Onufriev, A. *Proteins* **2006**, *63*, 928–938.
31. Guex, N.; Peitsch, M. C. *Electrophoresis* **1997**, *18*, 2714–2723. http://ca.expasy.org/spdbv/.
32. Sinnott, M. L.; Jencks, W. L. *J. Am. Chem. Soc.* **1980**, *102*, 2026–2032.
33. Gibson, R. P.; Turkenburg, J. P.; Charnock, S. J.; Lloyd, R.; Davies, G. J. *Chem. Biol.* **2002**, *9*, 1337–1346.